Analysis of optothermionic refrigeration based on semiconductor heterojunction

Peng Han, Kui-juan Jin,[a] Yueliang Zhou, and Xu Wang
Beijing National Laboratory for Condensed Matter Physics, Institute of Physics, Chinese Academy of Sciences, Beijing 100080, China

Zhongshui Ma
State Key Laboratory for Mesoscopic Physics, Peking University, Beijing 100871, China and Department of Physics, Peking University, Beijing 100871, China

Shang-Fen Ren
Department of Physics, Illinois State University, Normal, Illinois 61790-4560

A. G. Mal'shukov
Institute of Spectroscopy, Russian Academy of Sciences, 142092 Troitsk, Moscow Oblast, Russia

K. A. Chao
Division of Solid State Theory, Department of Physics, Lund University, S-223 62 Lund, Sweden

(Received 26 September 2005; accepted 24 February 2006; published online 10 April 2006)

We have examined the theory of optothermionic refrigeration combining the ideas of laser cooling and thermionic cooling [Mal'shukov and Chao, Phys. Rev. Lett. **86**, 5570 (2001)] and its estimation on thermal energy extraction by using self-consistent calculations with the drift-diffusion model in this paper. Both the Auger and the Shockley-Read-Hall dissipation processes are considered. For GaAs/AlGaAs systems with various impurity concentrations and different widths of quantum well, it is found that the optothermionic cooler can extract thermal energy at a rate as much as 10 W/cm^2. The information to perform optothermionic refrigeration in real devices have also been provided.
 [DOI: 10.1063/1.2188249]

I. INTRODUCTION

In a thermoelectric device, there exist both electric current and heat flow. While a spatial temperature gradient generates the useful electron current, the heat flow always tends to reduce the required temperature difference. The thermoelectric current and the heat backflow are the two key issues in the study of thermoelectric efficiency.

Because the dynamics of charge carriers, i.e., electrons or holes, is sensitive to electric field and magnetic field, it is easier to manipulate charge carriers than to manipulate phonons in a thermoelectric system. Consequently, the research and development of thermoelectricity have been focused on the electron subsystem. The early calculations of Ioffe, using a free electron gas model, suggested the doped semiconductors as the most favorable thermoelectric materials. However, the motion of electrons in a thermoelectric process is a diffusive transport due to various types of scattering. Hence, mechanisms and structures are needed in order to further improve the thermoelectric efficiency.

To go beyond the diffusive transport of electrons, one has to consider the ballistic motion, which was noticed by Thomas Edison in 1883 in connection with the thermal emission of electrons. Since Mahan proposed the thermionic refrigeration in a system with a vacuum gap between parallel metal electrodes,[1] various types of thermionic cooling devices have been proposed.[2–9] One basic problem in thermionic systems is the charge accumulation. Although attempts have been made to overcome this problem,[10–12] the expected efficiency of the thermionic devices has never been achieved.

Improving the intrinsic thermionic efficiency will only solve one problem of thermionic refrigeration. For a typical value of semiconductor thermal conductivity, when thermally excited carriers transfer heat from the cold region to the hot region, the opposite heat flow due to the lattice heat conduction tends to reduce the temperature difference. So, another approach is the fast extraction of heat from the system to be cooled. In conventional thermoelectric and/or thermionic coolers, if both electrons and holes participate in the transport process, they are separated spatially. A few years ago the optothermionic cooler was proposed,[13] which consisted of a narrow quantum well embedded in the middle of a *pn* junction. Electrons in the *n*-doped region and holes in the *p*-doped region are thermally excited into the quantum well, where they can recombine to emit light. Thus, the photons are mediums to extract the heat from the system. In this theory, the ideas of thermionic cooling and traditional laser cooling are combined to extract the thermionic heat from the system. So this method is called as *optothermionic refrigeration*. As pointed out in Ref. 13 the idea of cooling a *pn* junction with light emission was proposed about 40 years ago but has never been realized.

The optothermionic refrigerating system proposed in Ref. 13 has the typical heterostructure *p*-AlGaAs/AlGaAs/GaAs/AlGaAs/*n*-AlGaAs with 30% aluminum in the AlGaAs alloy. The impurity concentration is 10^{18} cm^{-3} for both the *p*-AlGaAs and the *n*-AlGaAs. The band-edge profile of

[a]Electronic mail: kjjin@aphy.iphy.ac.cn

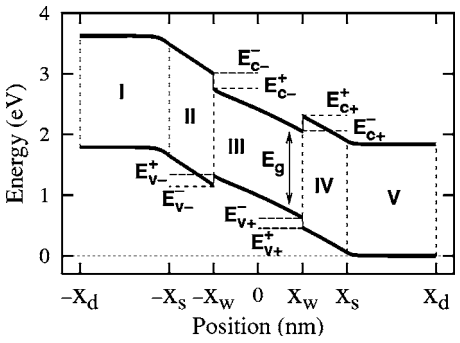

FIG. 1. The band-edge profile of a *p*-AlGaAs/AlGaAs/GaAs/AlGaAs/*n*-AlGaAs heterojunction with no bias ($V=0$) applied across the entire system between points x_d and $-x_d$. From region I to region V, the materials are *p*-AlGaAs, AlGaAs, GaAs, AlGaAs, and *n*-AlGaAs.

the system with no bias ($V=0$) applied is shown in Fig. 1. Region I is the *p*-AlGaAs and region V is the *n*-AlGaAs. Between the two regions II and IV of undoped AlGaAs lies the wide GaAs quantum well. When an electric current J flows through the system under a finite applied bias V, accompanying with the dissipation heat JV, an amount of radiation energy $Q_{\rm rad}$ is emitted from the GaAs quantum well. If $Q_{\rm rad}$ is larger than JV, the central region of the heterostructure is cooled down. Including the Auger recombination as the only nonradiative process, the energy difference $Q=Q_{\rm rad}-JV$, which is called as the *refrigeration heat* in this paper, was analyzed and estimated in Ref. 13. There it was shown that optothermionic cooling can be realized with proper choice of heterostructures.

In the semiquantitative analysis of Ref. 13, electrons and holes are assumed to be distributed uniformly in the quantum well. In such ideal systems, the optothermionic refrigeration can be achieved in a finite range of bias voltage, and the calculated cooling rate is at least several $\mathrm{W/cm^2}$. However, in a real system, both the carriers' transport process and recombination process are affected seriously by various factors, resulting in the nonuniform distribution of carriers. Thus for practical applications, we have calculated the optothermionic refrigeration self-consistently in this work.

In the present work the drift-diffusion model[14–17] is used to perform a self-consistent study on the refrigeration heat Q. Besides the radiative recombination, the Auger recombination and the Shockley-Read-Hall (SRH) recombination are also taken into account. The carrier distributions are calculated self-consistently with various bias voltages. This paper is organized as follows. The self-consistent scheme will be introduced in Sec. II. The recombination processes appearing in the set of self-consistent equations will be analyzed in Sec. III. Based on these self-consistent mathematical formulas, the optothermionic cooling phenomenon will be presented in Sec. IV, with numerical results for various impurity concentrations as well as different widths of the quantum well. For simplicity, the effect of the heat flow due to the lattice heat conduction is not considered in the present work. In Sec. V, we will discuss the conditions for realistic experiments on optothermionic refrigeration.

II. SELF-CONSISTENT ANALYSIS

There exist several numerical methods for analyzing the carrier transport in semiconductor heterostructures. Since in our system only thermally excited carriers can be driven into the quantum well, the suitable approach for this problem is to apply the drift-diffusion model[14–17] to each of the five regions shown in Fig. 1. Then, the Richardson current boundary condition[15] is imposed on the carrier transport across each of the interfaces at $x=-x_w$ and $x=x_w$.

To formulate a general analysis, let N_A^- be the ionized acceptor density in region I and N_D^+ the ionized donor density in region V. Throughout the entire system, $p(x)$ and μ_p [or $n(x)$ and μ_n] are the hole (or electron) density and mobility, respectively. Under the steady state, the electrostatic potential $\phi(x)$ and the recombination rate $R(x)$ satisfy the coupled equations

$$-\frac{d^2\phi(x)}{dx^2}=\frac{q}{\varepsilon}[p(x)-n(x)-N_A^-+N_D^+],$$

$$D_n\frac{d^2n(x)}{dx^2}-\mu_n\frac{d\phi(x)}{dx}\frac{dn(x)}{dx}-\mu_n n(x)\frac{d^2\phi(x)}{dx^2}=R(x),$$

$$D_p\frac{d^2p(x)}{dx^2}+\mu_p\frac{d\phi(x)}{dx}\frac{dp(x)}{dx}+\mu_p p(x)\frac{d^2\phi(x)}{dx^2}=R(x), \quad (1)$$

where q is the electron charge, ε the dielectric permittivity, D_n the electron diffusion coefficient, and D_p the hole diffusion coefficient. In the next section we will investigate in detail the recombination rate $R(x)$.

The current flowing across the interfaces at $x=-x_w$ and $x=x_w$ is of the thermionic nature. Therefore, we should apply the Richardson current boundary conditions[15] to these interfaces. Let us express the relevant effective Richardson constants of electrons and holes as[18,19] $A_{e-}^*=qm_{c-}^*k_B^2/2\pi^2\hbar^3$, $A_{e+}^*=qm_{c+}^*k_B^2/2\pi^2\hbar^3$, $A_{h-}^*=qm_{v-}^*k_B^2/2\pi^2\hbar^3$, and $A_{h+}^*=qm_{v+}^*k_B^2/2\pi^2\hbar^3$, with the corresponding electron (or hole) effective masses m_{c-}^* and m_{c+}^* (or m_{v-}^* and m_{v+}^*) in GaAs and AlGaAs, respectively. Then the electron current $J_n(x_w)$ at $x=x_w$ and the hole current $J_p(-x_w)$ at $x=-x_w$ can be written as

$$J_n(x_w)=A_{+e}^*T^2\exp\left(-\frac{E_{c+}^+-E_{fn}^+}{k_BT}\right)-A_{-e}^*T^2\exp\left(-\frac{E_{c+}^+-E_{fn}^-}{k_BT}\right), \quad (2)$$

$$J_p(-x_w)=A_{+h}^*T^2\exp\left(-\frac{E_{fp}^--E_{v-}^-}{k_BT}\right)-A_{-h}^*T^2\exp\left(-\frac{E_{fp}^+-E_{v-}^-}{k_BT}\right), \quad (3)$$

where the eight energies $E_{c\pm}^{\pm}$ and $E_{v\pm}^{\pm}$ are indicated in Fig. 1. E_{fn}^+ and E_{fn}^- are the quasichemical potentials of conduction band electrons at $x=-x_w$ in region IV and region III, respectively. Similarly, E_{fp}^+ and E_{fp}^- are the quasichemical potentials of valence band holes at $x=-x_w$ in region III and region II, respectively. To write down the exact expressions of these quasichemical potentials, let us define n_{c+}^+ (or n_{c+}^-) as the

electron density at $x=-x_w$ in regions IV and III, with the corresponding effective density of states ρ_{c+}^{+} (or ρ_{c+}^{-}). Then, we find in Ref. 17 that $E_{fn}^{\pm}=E_{c+}^{\pm}+k_BT\ln(n_{c+}^{\pm}/\rho_{c+}^{\pm})$. The similar expression for holes is $E_{fp}^{\pm}=E_{v+}^{\pm}+k_BT\ln(p_{v+}^{\pm}/\rho_{v+}^{\pm})$.

The validity of the above analysis imposes two conditions on the thickness x_s-x_w of the spacer layers. Since we have ignored the tunneling current through the triangle barrier, x_s-x_w must be longer than the carrier tunneling length which is typically 10 nm for $Al_{0.3}Ga_{0.7}As$ alloys. By assuming thermionic current over the triangle barrier, we must have x_s-x_w shorter than the carrier mean free path, which at room temperature in $Al_{0.3}Ga_{0.7}As$ alloy is about 100 nm.[20] Consequently, for our numerical calculation we have set the spacer thickness $x_s-x_w=50$ nm.

III. RECOMBINATION PROCESSES

To complete the self-consistent calculation in Eq. (1), it is very important to obtain the recombination rate $R(x)$. The dominating recombination processes in semiconductor,[21] the $R(x)$ term in Eq. (1), are the SRH recombination,[22] the Auger recombination,[23] and the radiative recombination.[24] These processes contribute differently in various regions of our system shown in Fig. 1 and will be analyzed as follows.

In an AlGaAs alloy, whether doped or not, the SRH recombination channel is important. In terms of electron concentration $n(x)$, hole concentration $p(x)$, electron lifetime τ_n, and hole lifetime τ_p, $R_{\mathrm{SRH}}(x)$ can be expressed as[14]

$$R_{\mathrm{SRH}}(x)=\frac{p(x)n(x)-n_i^2}{\tau_n[p(x)+n_i]+\tau_p[n(x)+n_i]}, \tag{4}$$

where n_i is the intrinsic carrier density and has a value of about 1.04×10^3 cm^{-3} in our system at room temperature. From Ref. 14, the lifetimes τ_n and τ_p are about 10^{-9} s.

In this quantum well, the Auger process and the radiative process compete against each other. The band structure of GaAs allows a large probability to transfer another hole within the valence band with the energy released from an electron-hole recombination. Therefore, the recombination is mainly the so-called conduction, hole, hole, split-off (CHHS) Auger process.[13,23,25,26] The corresponding recombination rate $R_{\mathrm{Aug}}(x)$ has the form[23]

$$R_{\mathrm{Aug}}(x)=\gamma[p^2(x)n(x)-p(x)n_i^2], \tag{5}$$

where γ is the Auger coefficient. In our system, the calculated value of γ is 6.5×10^{-30} cm^6/s.

In the quantum well the most important recombination for the optothermionic refrigeration is the radiative recombination.[13] Let E_g be the GaAs energy gap, and V_b the voltage drop across the quantum well between $x=-x_w$ and $x=x_w$. Then, the radiative rate $R_{\mathrm{rad}}(\hbar\omega_{\mathbf{k}}^{\lambda})$ for the photon with wave vector $\mathbf{k}$ and polarization λ can be written as[24]

$$R_{\mathrm{rad}}(\hbar\omega_{\mathbf{k}}^{\lambda})=\frac{q^2\eta\mu^{3/2}}{3\sqrt{2}\pi^3\varepsilon_0 m_0^2\hbar^5c^3}P_{cv}\hbar\omega_{\mathbf{k}}^{\lambda}\sqrt{\hbar\omega_{\mathbf{k}}^{\lambda}-E_g}\times\exp\left(\frac{qV_b-\hbar\omega_{\mathbf{k}}^{\lambda}}{k_BT}\right), \tag{6}$$

where m_0 is the electronic mass, η the refraction index, c the speed of light, and μ the electron-hole reduced effect mass. The momentum matrix element P_{cv} for the electron transition between the conduction and the valence band is calculated as

$$P_{cv}=-i\hbar\int_{-x_w}^{x_w}\psi_v^*(x)\frac{d}{dx}\psi_c(x)dx, \tag{7}$$

with the conduction band electron wave function $\psi_c(x)$ and the valence band hole wave function $\psi_v(x)$.

IV. OPTOTHERMIONIC REFRIGERATION

The optothermionic refrigeration consists of two competing processes: to heat up the system by energy dissipation within the sample and to cool down the system by removing the energy from the sample via light emission. Since the quantum well is made of pure GaAs and the spacer layers are very thin, in these regions the energy dissipation due to the SRH recombination process can be neglected. In a high quality pure semiconductor, only the band-to-band Auger recombination and the direct band-to-band radiative recombination are important.[13] Consequently, when an electric current J flows through the system, the dissipated heat can be written as

$$JV=qV\int_{-x_w}^{x_w}\left[R_{\mathrm{Aug}}(x)+\sum_{\lambda,\mathbf{k}}R_{\mathrm{rad}}(\hbar\omega_{\mathbf{k}}^{\lambda})\right]dx, \tag{8}$$

where V is the bias voltage applied to the entire system. The total energy carried out by photons, Q_{rad}, is simply

$$Q_{\mathrm{rad}}=\int_{-x_w}^{x_w}\sum_{\lambda,\mathbf{k}}\hbar\omega_{\mathbf{k}}^{\lambda}R_{\mathrm{rad}}(\hbar\omega_{\mathbf{k}}^{\lambda})dx. \tag{9}$$

Previously we have defined the *refrigeration heat* as

$$Q=Q_{\mathrm{rad}}-JV. \tag{10}$$

A positive value of Q indicates an effective optothermionic cooling. Inserting Eqs. (8) and (9) into Eq. (10) and performing relevant integrations, we obtain

$$Q=\left(\frac{q^2\eta\mu^{3/2}}{3\pi^2\sqrt{2\pi}\varepsilon_0 m_0^2\hbar^5c^3}\right)P_{cv}^2E_g(k_BT)^{3/2}\exp\left(\frac{qV_b-E_g}{k_BT}\right)\times\left[E_g+3k_BT+\frac{15(k_BT)^2}{4E_g}-qV\left(1+\frac{3k_BT}{2E_g}\right)\right]-qV\int_{-x_w}^{x_w}R_{\mathrm{Aug}}(x)dx. \tag{11}$$

With these formulas and the $GaAs/Al_{0.3}Ga_{0.7}As$ heterostructure shown in Fig. 1, we have performed a numerical study on the optothermionic phenomenon at room temperature of $T=300$ K. The necessary parameters for our calculations can be found in Refs. 14 and 21. For undoped semiconductor materials, the mobility of electrons is 8000 cm^2/(V s) in GaAs and 2500 cm^2/(V s) in $Al_{0.3}Ga_{0.7}As$, while that of holes is 400 cm^2/(V s) in GaAs and 150 cm^2/(V s) in $Al_{0.3}Ga_{0.7}As$. For the highly doped (about 10^{18} cm^{-3}) $Al_{0.3}Ga_{0.7}As$, the electron mobility is taken as 800 cm^2/(V s) and that of holes is taken as 75 cm^2/(V s).

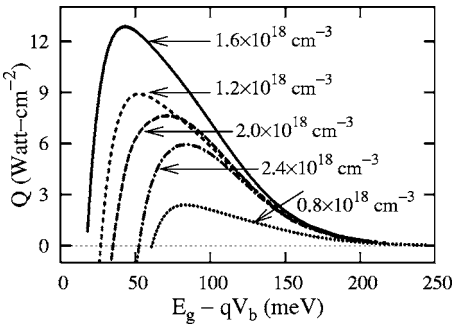

FIG. 2. Refrigeration heat as a function of $E_g - qV_b$ for different impurity concentrations marked next to the corresponding curves. The width of the quantum well is 100 nm.

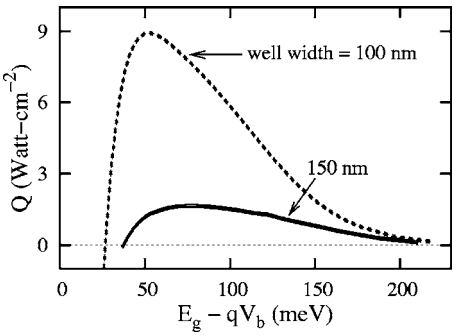

FIG. 4. Refrigeration heat as a function of $E_g - qV_b$ for quantum well widths of 100 nm (dotted curve) and 150 nm (solid curve) with the same impurity concentration of 1.2×10^{18} cm^{-3}.

The electron diffusion coefficient D_n and the hole diffusion coefficient D_p are calculated with $D_n = k_B T \mu_n / q$ and $D_p = k_B T \mu_p / q$.

We have set $x_w = 50$ nm, $x_s = 100$ nm, and $x_d = 200$ nm to specify the layer thickness in Fig. 1. To make it easier to present our numerical results, in our calculations we have used the same donor concentration and acceptor concentration, which we call the impurity concentration N_{imp}. For a given N_{imp}, we have calculated the refrigeration heat Q as a function of the applied bias voltage V. However, we will first analyze Q as a function of $E_g - qV_b$, where V_b is the bias on the well and is derived from the corresponding V. The result is shown in Fig. 2 for various values of N_{imp}. In the region of large values of $E_g - qV_b$, Q drops exponentially as predicted in Eq. (11).

For a given value of N_{imp}, Q has a maximum value $Q_{\max}(N_{\text{imp}})$. As N_{imp} gets larger, this peak value $Q_{\max}(N_{\text{imp}})$ first increases and then decreases. To find out the origin of such a behavior, we plot in Fig. 3 the electron spatial density $n(x)$ and the hole spatial density $p(x)$ corresponding to $Q_{\max}(N_{\text{imp}})$ for $N_{\text{imp}} = 1.2 \times 10^{18}$ cm^{-3} (dashed curves), 1.6×10^{18} cm^{-3} (solid curves), and 2.0×10^{18} cm^{-3} (dotted curves). We notice that the carrier densities have smallest values for $N_{\text{imp}} = 1.2 \times 10^{18}$ cm^{-3} and have largest spatial polarization for $N_{\text{imp}} = 2.0 \times 10^{18}$ cm^{-3}. Both of these can reduce the radiative recombination rate. Therefore, the high radiative recombination rate for $N_{\text{imp}} = 1.6 \times 10^{18}$ cm^{-3} yields its largest value of $Q_{\max}(N_{\text{imp}})$.

Since $Q_{\max}(N_{\text{imp}})$ depends on the carrier spatial distributions $n(x)$ and $p(x)$, we expect to observe the dependence of Q on the quantum well width $2x_w$. We have performed similar calculation for two wells with widths $2x_w = 100$ nm and $2x_w = 150$ nm with the same impurity concentration $N_{\text{imp}} = 1.2 \times 10^{18}$ cm^{-3}. The calculated Q is shown in Fig. 4, and the corresponding spatial distribution of carrier density in Fig. 5. In the wider quantum well, the carrier densities are reduced and the spatial distribution of carriers is polarized, thus the refrigeration heat Q for the wider quantum well is much smaller than that of the narrower quantum well.

It should be noticed that the width of the well should not be decreased infinitely for a realistic system because the model of the bulk Auger recombination will not be right with the width less than a threshold value (about 100 nm for GaAs). In that case, we will have to use *thresholdless* or *quasithreshold* model of Auger process,[13,25,26] in which the Auger recombination rate will be much larger than that of bulk model.

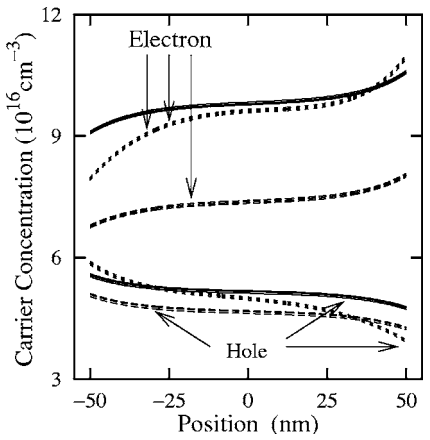

FIG. 3. Spatial distribution of electron and hole density for the impurity concentrations $N_{\text{imp}} = 1.2 \times 10^{18}$ cm^{-3} (dashed curves), 1.6×10^{18} cm^{-3} (solid curves), and 2.0×10^{18} cm^{-3} (dotted curves). The width of the quantum well is 100 nm.

V. SUMMARY

Even though the optothermionic theory[13] gave an estimate of the value of the refrigeration heat Q, the conditions under which this theory is valid have been uncertain. In the

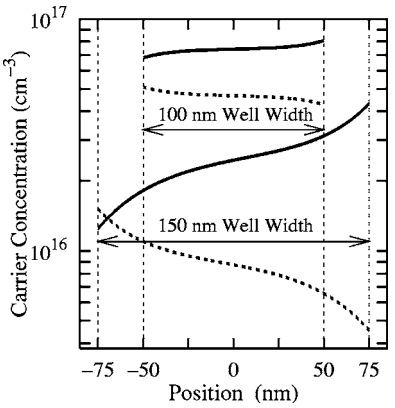

FIG. 5. Spatial distribution of electron and hole density for quantum well widths of 100 nm (dotted curve) and 150 nm (solid curve) with the same impurity concentration of 1.2×10^{18} cm^{-3}.

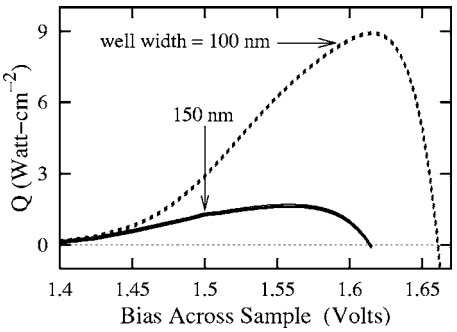

FIG. 6. Refrigeration heat as a function of voltage for quantum well widths of 100 nm (dotted curve) and 150 nm (solid curve) with the same impurity concentration of 1.2×10^{18} cm^{-3}.

present work, we have given a detailed analysis with a reliable self-consistent numerical method and confirmed the prediction of the optothermionic theory. From our calculation, the refrigeration heat not only changes with doping density, applied bias voltage, but also increases with decreasing the well width. For a well width of 100 nm, we have found that the proper parameters to obtain the most efficient refrigeration are doping density of 1.6×10^{18} cm^{-3} and bias voltage of about 1.6 V. These results have directive meaning for realizing optothermionic refrigeration. In real experiments, one applies the bias V over the entire system. Although the plots of Q vs E_g-qV_b provides a better way to understand the physical processes, as shown in Figs. 2 and 4, it will be very informative to the experimentalists for performing their experiments if we plot Q as a function of V. For this purpose, in Fig. 6 we present the same data as in Fig. 4, but using the applied bias V as the horizontal axis. This result indicates that real experiments of optothermionic refrigeration can be realized at room temperature. We should point out that in a real device, the process of emitting recombined photons from the system is limited by the light emitting efficiency of the quantum well. In addition, the radiative recombination rate in the quantum well can be reduced by the optical absorption process. Therefore, the optothermionic refrigeration efficiency in a real device will be less than that of the theoretical result. So it would be interesting in further study to find out methods for increasing the light emitting efficiency and decreasing the optical absorption rate.

ACKNOWLEDGMENTS

This work was supported by the National Natural Science Foundation of China, and the SIDA-Swedish Research Links Grant No. 348-2002-6935.

[1]G. D. Mahan, J. Appl. Phys. **76**, 4362 (1994).
[2]G. D. Mahan and L. M. Woods, Phys. Rev. Lett. **80**, 4016 (1998).
[3]L. D. Hicks, T. C. Harman, and M. S. Dresselhaus, Appl. Phys. Lett. **63**, 3230 (1993).
[4]X. Sun, Z. Zhang, and M. S. Dresselhaus, Appl. Phys. Lett. **74**, 4005 (1999).
[5]A. Shakouri and J. E. Bowers, Appl. Phys. Lett. **71**, 1234 (1997).
[6]A. Shakouri, C. LaBounty, J. Piprek, P. Abraham, and J. E. Bowers, Appl. Phys. Lett. **74**, 88 (1999).
[7]X. Fan *et al.*, Appl. Phys. Lett. **78**, 1580 (2001).
[8]D. Vashaee and A. Shakouri, J. Appl. Phys. **95**, 1233 (2004).
[9]D. H. Huang, T. Apostolova, P. M. Alsing, and D. A. Cardimona, Phys. Rev. B **70**, 033203 (2004).
[10]R. J. Radtke, H. Ehrenreich, and C. H. Grein, J. Appl. Phys. **86**, 3195 (1999).
[11]C. B. Vining and G. D. Mahan, J. Appl. Phys. **86**, 6852 (1999).
[12]M. D. Ulrich, P. A. Barnes, and C. B. Vining, J. Appl. Phys. **90**, 1625 (2001).
[13]A. G. Mal'shukov and K. A. Chao, Phys. Rev. Lett. **86**, 5570 (2001).
[14]K. Horio and H. Yanai, IEEE Trans. Electron Devices **37**, 1093 (1990).
[15]M. S. Lundstrom and R. J. Schuelke, IEEE Trans. Electron Devices **30**, 1151 (1983).
[16]B. M. Grossman and M. J. Hargrove, IEEE Trans. Electron Devices **30**, 1092 (1983).
[17]J. E. Sutherland and J. R. Hauser, IEEE Trans. Electron Devices **24**, 363 (1977).
[18]K. Yang, J. R. East, and G. I. Haddad, Solid-State Electron. **36**, 321 (1993).
[19]K. Yang, J. R. East, and G. I. Haddad, IEEE Trans. Electron Devices **41**, 138 (1994).
[20]A. G. Mal'shukov, Z. Ma, V. B. Antonyuk, and K. A. Chao, Solid State Commun. **119**, 563 (2001).
[21]D. A. Neamen, *Semiconductor Physics and Devices Basic Principles*, 3rd ed. (McGraw-Hill, New York, 2003).
[22]W. Shockley and W. T. Read, Phys. Rev. **87**, 835 (1952).
[23]V. N. Abakumov, V. I. Perel, and I. N. Yassievich, *Nonradiative Recombination in Semiconductors* (North-Holland, Amsterdam, 1991).
[24]B. K. Ridley, *Quantum Processes in Semiconductors* (Clarendon, Oxford, 1982).
[25]A. S. Polkovnikov and G. G. Zegrya, Phys. Rev. B **58**, 4039 (1998).
[26]M. I. Dyakonov and V. Yu. Kachorovskii, Phys. Rev. B **49**, 17130 (1994).